An isotopic analysis of geothermal brine and calcite scaling from the Blue Mountain geothermal field, Winnemucca, Nevada

Christopher French

A report prepared in partial fulfillment of
The requirements for the degree of

Master of Science
Earth and Space Sciences: Applied Geosciences

University of Washington

March 2016

Project mentor:
Trenton Cladouhos, AltaRock Energy, Inc.

Internship coordinator:
Kathy Troost

Reading committee:
Katharine Huntington
Juliet Crider

MESSAGe Technical Report Number: 029

Abstract

Understanding, and controlling, the conditions under which calcite precipitates within geothermal energy production systems is a key step in maintaining production efficiency. In this study, I apply methods of bulk and clumped isotope thermometry to an operating geothermal energy facility in northern Nevada to see how those methods can better inform the facility owner, AltaRock Energy, Inc., about the occurrence of calcite scale in their power plant. I have taken water samples from five production wells, the combined generator effluent, shallow cold-water wells, monitoring wells, and surface water. I also collected calcite scale samples from within the production system. Water samples were analyzed for stable oxygen isotope composition ($\delta^{18}O$). Calcite samples were analyzed for stable oxygen and carbon ($\delta^{13}C$) composition, and clumped isotope composition (Δ_{47}). With two exceptions, the water compositions are very similar, likely indicating common origin and a well-mixed hydrothermal system. The calcite samples are likewise similar to one another. Apparent temperatures calculated from $\delta^{18}O$ values of water and calcite are lower than those recorded for the system. Apparent temperatures calculated from Δ_{47} are several degrees higher than the recorded well temperatures. The lower temperatures from the bulk isotope data are consistent with temperatures that could be expected during a de-pressurization of the production system, which would cause boiling in the pipes, a reduction in system temperature, and rapid precipitation of calcite scale. However, the high apparent temperature indicated by the Δ_{47} data suggests that the calcite is depleted in clumped isotopes given the known temperature of the system, which is inconsistent with this hypothesis. This depletion could instead result from disequilibrium isotopic fractionation during the aforementioned boil events, which would make both the apparent $\delta^{18}O$-based and Δ_{47}-based temperatures unrepresentative of the actual water temperature. This research can help improve our understanding of how isotopic analyses can better inform us about the movement of water through geothermal systems of the past and how it now moves through modern systems. Increased understanding of water movement in these systems could potentially allow for more efficient utilization of geothermal energy as a renewable resource.

ntTable of Contents

Table of Contents

List of Figures

List of Tables

Acknowledgements

1 Introduction

Calcite deposition within geothermal energy production facilities is problematic because it reduces the efficiency of the production system (Satman et al., 1999). The determination of calcite precipitation conditions may further aid geothermal companies in controlling calcite formation. Calcite-water oxygen isotope thermometry is a well-established field used to estimate the temperature of calcite precipitation based on the enrichment of heavy oxygen isotopes in calcite and the water from which the mineral precipitated (Epstein and Mayeda, 1953; McCrea, 1950; Urey, 1947). Clumped isotope (Δ_{47}) thermometry is a newer method used to estimate calcite precipitation temperature independently of the isotopic composition of the water from which the mineral grew, based on the enrichment of "clumped" molecules containing both heavy isotopes of oxygen and carbon (^{18}O and ^{13}C) in calcite relative to a stochastic distribution of isotopes (Eiler, 2007; Ghosh et al., 2006). If calcite precipitates in isotopic equilibrium, both methods should produce temperature estimates that agree with each other and accurately reflect the temperature of the geothermal water from which the mineral grew—providing potentially useful information on past fluid temperatures and calcite growth conditions in geothermal systems. Here, I applied these two methods of isotopic thermometry to modern samples collected in a well-monitored geothermal system to determine if the calcite precipitated at equilibrium or if the resulting temperature predictions differ from each other and also from the observed state of the system.

Geothermal water (referred to as "brine") and modern calcite deposits were sampled at a geothermal energy production facility at Blue Mountain, near Winnemucca, Nevada (Figure 1). Samples were analyzed using isotope ratio mass spectrometry to quantify the stable and clumped isotope compositions of calcite, and cavity ring-down spectroscopy to quantify the stable isotope composition of geothermal brine. The data were used to calculate apparent calcite precipitation temperatures, which were compared to the measured water temperature in the geothermal wells to determine whether or not calcite precipitated at isotopic equilibrium in this geothermal system. This research can also help improve our understanding of how isotopic analyses can better inform us about the movement of water through geothermal systems of the past and how it now moves through modern systems. Increased understanding of water movement in these systems

could potentially allow for more efficient utilization of geothermal energy as a renewable resource.

2   Scope of Work

In order to better understand how stable and clumped isotope geochemistry can be used to help characterize geothermal systems, I have done the following:

- Conducted a literature review of materials relating to the Blue Mountain geothermal field, calcite formation, isotopic data for surface water in the region, and clumped isotope thermometry.
- Collected thirteen water samples from five geothermal production wells, two shallow cold water wells, three monitoring wells, geothermal production effluent, and surface water from within the Blue Mountain geothermal field.
- Collected ten calcite samples from material precipitated inside the geothermal production system and one sample from material precipitated on the outside of a leak in one well's pump housing.
- Analyzed calcite for stable isotope values of $\delta^{18}O$, $\delta^{13}C$, and Δ_{47} to determine formation temperature and calculate the expected $\delta^{18}O$ value of parent water.
- Analyzed water $\delta^{18}O$ values, (1) for comparison with values calculated from calcite $\delta^{18}O$ values, and (2) to compare among water samples to evaluate the homogeneity of the aquifer system.

3   Background

3.1   The Blue Mountain Geothermal Field

The Blue Mountain geothermal basin is located along the Luning-Fencemaker fold-and-thrust belt within the Basin and Range Province in northwestern Nevada (Figure 2. Geology and general structure in the vicinity of Blue Mountain. (Wyld, 2002).; Wyld, 2002). The Basin and Range province is characterized by northwest-southeast Miocene extension; in the Luning-Fencemaker fold-and-thrust belt, including Blue Mountain experienced 55% to 75% northwest-southeast shortening during the Mesozoic (Wyld, 2002). Crustal shortening is evidenced by the prominent northeast-trending structural grain—primarily isoclinal folding at various scales, wide

spread cleavage, and reverse faulting. Crustal thinning associated with the more recent extension of the Basin and Range increased the surface proximity to the mantle, steepening the geothermal gradient. In the Blue Mountain basin, the local geology comprises Triassic pelitic metasedimentary rocks; including argillite, slate, phyllite, and lesser interbedded quartzite (Faulds and Melosh, 2008). Prominent faulting associated with the Luning-Fencemaker fold-and-thrust belt has allowed water to percolate into the relatively shallow thermal zone and reach temperatures nearing 200°C (AltaRock Energy, Inc., 2014).

The primary geothermal aquifer exists along a series of west-dipping faults (Figure 3; AltaRock Energy, Inc., 2014). Wells screened in this aquifer range in depth from 2,700 ft to 6,600 ft (all well depths courtesy of AltaRock Energy, Inc.). A shallower, cold aquifer is situated at approximately 90 ft to 300 ft (according to well screen data courtesy of AltaRock Energy, Inc.).

3.2   Geothermal power production at Blue Mountain

A geothermal power plant is currently in operation in the geothermal field owned by AltaRock Energy, Inc. and operated by Nevada Geothermal Power, Inc. (NGP). The plant was built in 2009 with a designed production capacity of 50 MW. At the time the plant was built, geothermal production well temperatures were as high as 200 °C. Since energy production began, production temperatures have dropped to an average of 164 °C. Production has since declined to approximately 29 MW due to declining geothermal temperatures (AltaRock Energy, Inc., 2014). AltaRock purchased the facility in 2015 to begin exploring ways in which production could be increased.

NGP runs five production wells in the center of the field and seven injection wells around the western perimeter (Figure 1). Two water wells, screened in the shallow aquifer provide water for general plumbing and for cooling the plant.

The plant operates by evaporating isopentane with hot geothermal brine, such that the evaporated isopentane powers turbines that generate electricity (Figure 4). The 164°C brine is pumped from the geothermal reservoir at the five production wells. The flows are combined and then divided among three power generators. Once in the generators, heat from the brine is used to evaporate isopentane which has a boiling point of 28°C. Isopentane vapor turns the turbines, generating electricity. The water leaves the generators through a combined outflow and then is split among

the seven injection wells, which pump the water back into the geothermal aquifer to replenish the geothermal resource.

The entire production system is kept under pressure in order to prevent boiling and reduce calcite precipitation, known as scale. If uncontrolled, scale deposits can greatly reduce plant efficiency by choking the flow of water through the system. Efficiency is also affected when scale breaks free from the inside of the pipes carrying the brine to the generators and then enters the generators. Periodically, plant shutdowns occur due to system malfunction or for maintenance. During these shutdowns positive pressure is lost, boiling occurs, and an increase in calcite scaling is observed (Ed Smirnes, personal communication, February 4, 2016). A filter screen was installed in line before the third generator after AltaRock determined that the generator's efficiency was being impacted by loose scale entering the turbine.

AltaRock is actively studying the geochemistry of the Blue Mountain geothermal system to improve production at this site, and to advance general understanding of geothermal systems. NGP regularly samples water from four monitoring wells spread across the field in order to keep track of the water chemistry of the system and to ensure compliance with Environmental Protection Agency (EPA) clean water standards. As such, there is a wealth of information available about the geochemistry of the system from ongoing sampling and monitoring efforts. Prior work on the isotope geochemistry of calcite at Blue Mountain includes a study by Sumner et al. (2015). They used stable and clumped isotope analyses to estimate past reservoir temperatures based on calcite veins from rock cores collected during well-drilling at the site.

3.3   Conventional δ^{18}O and clumped isotopes thermometry in calcites

Calcium carbonate, $CaCO_3$, or calcite, is a common mineral in hydrogeological systems. This is due to its relatively high solubility in water. Calcite precipitation in geothermal systems can be driven by hydrolysis (mineral replacement reactions), liquid to gas phase changes, and increased temperature (inverse solubility) (Simmons and Christenson, 1994). As calcite precipitates, the common, light carbon and oxygen atoms (^{12}C and ^{16}O) within the mineral may be substituted with rare, heavy carbon and oxygen isotopes (^{13}C and ^{17}O or ^{18}O; e.g. Eiler, 2007). If the calcite precipitates in isotopic equilibrium, the ratio of ^{18}O to ^{16}O in the calcite, which is described by the δ^{18}O value (δ^{18}O = [^{18}O/^{16}O$_{sample}$ ÷ ^{18}O/^{16}O$_{standard}$ − 1] ×1000), depends on both the temperature of mineral growth and the δ^{18}O of the water from which the mineral precipitated

(Urey, 1947; McCrea, 1950; Epstein and Mayeda, 1953). The amount of enrichment of one isotope to another during precipitation is known as isotope fractionation. The process leading to precipitation influences the extent of fractionation, which can be expressed by a fractionation factor (α), defined as the factor by which the abundance ratio of two isotopes will change during a chemical reaction or a physical process (e.g., Kim and O'Neil, 1997). Empirical relationships have been used to calculate the precipitation temperature of calcite based on the $\delta^{18}O$ value of the calcite and $\delta^{18}O$ value of the water from which it precipitated (e.g., Kim and O'Neil, 1997; Eq. 1):

$$1000 \ln \alpha = 18.03(10^3 T^{-1}) - 32.42 \tag{1}$$

In geothermal systems, most calcite precipitation is controlled by $f CO_2$ (e.g. Browne and Ellis, 1970). The reaction between geothermal brine, calcite ($CaCO_3$), and CO_2 can be generally described by the equation:

$$2HCO_3^- + Ca^{++} = CaCO_3 + H_2O + CO_2 \tag{2}$$
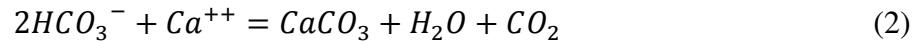
When brine boils, as occasionally happens in geothermal energy production systems, CO_2 is released from solution, forcing the reaction to the right.

The abundance of calcite molecules that contain both a heavy isotope of carbon (^{13}C) and of oxygen (^{18}O) "clumped" in the same molecule, in excess of what would be expected to occur by random chance, depends only on the temperature of mineral growth (Ghosh et al., 2006; Schauble et al., 2006; Eiler, 2007). Both the "bulk" isotopic composition ($\delta^{18}O$ value and $\delta^{13}C$ value, which is defined as $\delta^{13}C = [^{13}C/^{12}C_{sample} \div {}^{13}C/^{12}C_{standard} - 1] \times 1000$) and clumped isotope composition of calcite are measured by mass spectrometry of CO_2 produced by digesting the calcite in phosphoric acid; mass-47 CO_2 is mostly a measure of the clumped molecule $^{13}C^{18}O^{16}O$, and the Δ_{47} value is used to describe the observed $^{13}C^{18}O$ clumping in excess of the random distribution (Eiler and Schauble, 2004).

A major limitation of calcite $\delta^{18}O$ thermometry is that it requires information on the $\delta^{18}O$ composition of the water from which the calcite precipitated. Though not an issue when studying modern systems in which both water and calcite can be sampled, the need for information on the water makes these methods unworkable when studying systems which no longer have water or in which the water geochemistry has changed significantly since the calcite precipitated. The use of

clumped isotopes circumvents this problem. The proportion of clumped ^{18}O and ^{13}C isotopes in carbonates beyond the amount predicted by random distribution is temperature dependent (Ghosh et al., 2006; Schauble et al., 2006; Eiler, 2007), assuming the carbonate precipitated in isotopic equilibrium with its parent fluid. By analyzing for the enrichment in the calcite of molecules containing ^{13}C-^{18}O clumps, the precipitation temperature of the carbonate can be determined as follows:

$$\Delta_{47} = 0.405(\pm 0.004) \cdot \left(\frac{10^5}{T^2}\right) + 0.167(\pm 0.002) \tag{3}$$

Where T is in kelvin. This temperature calibration, developed by Kluge et al. (2015), is based on empirical data combined with the data of Dennis and Schrag (2010), Passey and Henkes (2012), and Tang et al. (2014). Of the many temperature calibration equations, Eq. 3 is the most appropriate for this study because (1) it is one of the few calibrations developed over a temperature range that applies to geothermal systems (25 to 250 °C), and (2) the methods of analysis used in this study (section 4.2.3; methods of Burgener et al., in press) are most similar to those of Kluge et al. (2015).

4 Methods

The following sections outline my field sampling methods, the methods I used to analyze my samples, and the calculations I used to predict temperatures based on the isotopic data. In addition to my samples and analyses, I received temperature data for the plant from AltaRock. AltaRock monitors system temperatures via thermocouples located at each of the production well-heads and the combined plant inflow and outflow (immediately before and after the generators).

4.1 Sampling methods

With the assistance of the facility staff, I collected thirteen water samples, one each from the five active geothermal production wells (14-14, 17-14, 23-14, 25-14, and 26A-14), two active cooling water wells (WW8 and WW14), four monitoring wells (MW5, MW6, MW7, and WW5), the common injection line, and one from a puddle presumed to have formed from rainwater (Figure 1). All water was collected in HDPE plastic bottles (sizes are described below). In addition to the water samples, I collected eleven calcite samples, ten from a collection of loose chips of calcite scale filtered from the production system and one from a mass of material precipitated on the

exterior of a pump housing. All calcite samples were collected in Ziploc-style plastic bags. All water and calcite samples were collected in December, 2015.

For the production wells, water was sampled from a sample valve approximately 30 feet downstream from the well head. A cooling coil in a 25 gallon bucket of cold water was attached to the valve in order to cool the water to a manageable handling temperature without allowing for evaporation (Figure 5). The sample containers were rinsed with the sample water prior to filling. At each production well I collected one 1 liter bottle and two 60 mL bottles to allow for test duplicates if necessary.

The common injection line, which carries the combined effluent from all five production wells after the water has passed through the power generators, was sampled from a sampling valve located approximately 100 ft down flow from the generators. One 60 mL bottle was collected at this location.

As with the common injection line, cooling water wells were sampled directly from sample valves into 60 mL bottles.

Monitoring wells were sampled using bladder pumps. Each well was purged for approximately 10 minutes prior to sampling to ensure water was representative of the formation water. One 60 mL sample was collected at each of the monitoring wells.

A puddle presumed to consist of rainwater was sampled by immersing a 250 mL bottle in the puddle, rinsing once, and then collecting the sample. At the time of sampling, the puddle measured approximately 15 ft by 8 ft at its widest points and less than 8 inches deep at the deepest point. Trace precipitation was recorded during several precipitation events in the weeks prior to sampling that could have contributed to the puddle (The Weather Company, 2016).

For all water samples, I measured pH and temperature in the field using a Mettler Toledo FG2 FiveGo Portable pH meter (pH accuracy quoted by the manufacturer of ±0.01).

Ten chips of calcite scale (Figure 6) were collected from a drum of material removed from the filter screen that prevents loose scale material from entering the power generators. The filter screen is cleaned periodically and emptied into the drum. As mentioned previously, because the

filter is situated after the pipes flowing from the five production wells have been combined into a single flow, the specific source location of each chip along the pipeline is not known.

One calcite sample was collected from material that had precipitated on the exterior of the pump apparatus at well 14-14, around a leak (Figure 7).

Water and calcite were kept under refrigeration until delivery to the University of Washington where they were kept in a walk-in freezer until the analyses were performed. Water samples were kept frozen to reduce the potential for post-sampling isotopic fractionation. Calcite samples were stored in the freezer with the water as a matter of convenience.

4.2   Analytical methods

All analyses were performed at the University of Washington IsoLab in the Department of Earth and Space Sciences. Descriptions of the analyses performed on the samples are detailed in sections 4.3.1 through 4.3.4 below.

4.2.1   *Water stable isotopes*

All thirteen water samples were analyzed for $\delta^{18}O$ using a Picarro L2120i cavity ring-down spectrometer (Gupta et al., 2009). This equipment measures spectral absorption of water vapor from the samples, from which $\delta^{18}O$ values are derived. Water samples were referenced to the Vienna Mean Ocean Water (VSMOW; Coplen, 1993) scale using two bracketing internal reference waters.

4.2.2   *Calcite bulk stable isotopes*

Twenty-one calcite samples were analyzed for stable isotope values of $\delta^{18}O$ and $\delta^{13}C$. These include twenty samples of calcite collected from the front and back (flow side and pipe side) of ten chips of calcite scale retrieved from the filter screen and one sample collected from calcite precipitated on the outside of pump 14-14. Isotopic measurements from both sides of the calcite filter screen samples were made in order to assess whether the samples were precipitated as single or multiple generations. Differing isotopic compositions from the same sample would imply that the calcite was precipitated during more than one stage. The scale samples were removed from the scale chips using a rotary drill tool. The samples (approximately 100μg each) were analyzed using a Kiel III carbonate device coupled to a Finnigan Delta Plus isotope ratio mass spectrometer using the methods of Tobin et al. (2011). This analysis also yields the percent

carbonate of the samples, allowing for the selection of samples that would be most suitable for Δ_{47} analysis.

4.2.3 Calcite clumped isotopes

Scheduling constraints with the preparation line prevented us from analyzing all eleven of the original field samples. Due to the large sample size requirements for Δ_{47} analysis (6-8 mg per analysis with three replicate analyses per sample), ideal candidates for Δ_{47} analysis were judged to be those that exhibited the highest percent of calcite and also homogeneity between front and back of the scale chip, implying a single generation of calcite precipitation. Two scale samples, SC03 and SC05, were chosen for Δ_{47} analysis. I removed three replicate subsamples from each chip, three being the minimum number recommended for this analysis, using a rotary drill tool. The samples were digested in a 90°C phosphoric acid (H_2PO_4) bath to produce CO_2. After being purified by subjection to multiple cryogenic traps and a Porapak Q trap, the CO_2 samples were analyzed using a Thermo MAT253 isotope ratio mass spectrometer following the methods of Burgener et al. (in press).

4.3 Thermometry Calculations

The fractionation factor equation of Kim and O'Neil (1997; Eq. 1) was used to calculate the apparent calcite precipitation temperature based on $\delta^{18}O$ results for water and calcite. $1000\ln\alpha$ is equal to the $\delta^{18}O$ value of the calcite minus the $\delta^{18}O$ value of the parent water (each as referenced to VSMOW) and T is in kelvins. The Δ_{47}-temperature calibration equation of Kluge et al. (2015), Eq. 3, was used to calculate the apparent calcite precipitation temperature based on the Δ_{47} results.

5 Results

5.1 Water stable isotopes, pH, and temperature

The $\delta^{18}O$ values of the water samples range from -15.3 to -13.9 ‰ with the exception of two samples, MW6 and the puddle, which have significantly higher $\delta^{18}O$ values of -7.6 to -6.7 ‰ (**Error! Reference source not found.**). MW6 is one of the monitoring wells (Figure 1); the depth of this well could not be determined at the time this report was prepared. Given that the puddle is most likely sourced from meteoric water; the similarity between the $\delta^{18}O$ value of MW6 and that of the puddle suggests that MW6 may be influenced by surface water infiltration.

The average $\delta^{18}O$ value for precipitation in the area is -11 ± 1 ‰ (IAEA/WMO, 2016), ~4 ‰ lower than the MW6 and puddle sample $\delta^{18}O$ values. The average $\delta^{18}O$ value of the remaining samples is -14.7 ‰ with a standard deviation of 0.5 ‰. The group of more ^{18}O depleted samples includes the five production wells, the common injection pipeline, two cooling water wells screened in the shallow aquifer, and three monitoring wells.

The pH values for all of the water samples ranged from 5.70 to 8.43. The average was 6.3 with a standard deviation of 0.8.

5.2   Calcite bulk stable isotopes

All but one of the samples are pure (100 %) calcite. Sample 14-14, collected from the exterior of well pump 14-14, is only 20 % calcite, and therefore the measured $\delta^{13}C$ and $\delta^{18}O$ values of 14-14 likely contain considerable instrumental error as the CO_2 yield during acid digestion was too low; the sample had low carbonate content but the same sample mass was used as the pure calcite samples. Calcite sample 14-14 will not be discussed further in this report (Appendix I)

The remaining $\delta^{13}C$ and $\delta^{18}O$ values of the calcite scale samples show remarkable consistency among the samples (**Error! Reference source not found.**). Because the values reported for the front and back of each scale filter screen sample are not significantly different, they have been treated as replicates of the scale chip from which they were derived. For the scale samples, the $\delta^{13}C$ values range from -8.6 to -8.1 ‰. The $\delta^{18}O$ values range from -34.2 to -32.7 ‰.

5.3   Calcite clumped isotopes

The subset of samples selected for clumped isotope analysis yield Δ_{47} values of 0.344 ± 0.015 ‰ and 0.360 ± 0.018 ‰ (1 standard error for three replicates) for samples SC03 and SC05, respectively (Table 2). These values are reported in the Absolute Reference Frame (ARF; Dennis et al., 2011). Apparent temperatures calculated from these Δ_{47} values using the calibration of Kluge et al. (2015; Eq. 3) are 205 ± 27 °C and 186 ± 28 °C (95 % confidence, including both analytical error and calibration uncertainties). Our results confirm that this is the most appropriate calibration to use because it ranges from 25 to 250 °C, encompassing the temperature range of our samples.

6 Discussion

6.1 Water $\delta^{18}O$ values

The small degree of variation in $\delta^{18}O_{water}$ values among all but one of the sampled well waters is consistent with the results of tracer testing done by AltaRock (AltaRock Energy, Inc., 2014) that indicate a well-mixed system. The average $\delta^{18}O$ value of the wells is ~ -14.7 ‰, which is ~4 ‰ lower than the average reported precipitation value for the area (-11±1 ‰; IAEA/WMO, 2016). This suggests that the shallow aquifer and wells have an ^{18}O-depleted meteoric source, potentially reflecting isotopically light recharge from high elevation. The $\delta^{18}O$ value of puddle water (-6.69±0.04 ‰) is ~4 ‰ higher than the average reported precipitation value for the area. Given the infrequent nature and small scale of recent precipitation events (The Weather Company, 2016), the puddle water was likely enriched in ^{18}O due to evaporation. One possible explanation for MW6 sample being so similar to the puddle sample and not to the other wells is that it is situated in close proximity to two infiltration ponds that are used to dispose of excess water not pumped to the injection wells. It could be that MW6 $\delta^{18}O$ values reflect the influence of these ponds which would have experienced the same evaporative enrichment in ^{18}O as the puddle. However, the similarity of the $\delta^{18}O$ values of MW6 and the puddle does not necessarily mean that the well from which MW6 was sampled contains evaporatively enriched meteoric water. Given the other evidence for a well-mixed system, it is possible that higher $\delta^{18}O$ value of MW6 water reflects a higher degree of fluid-rock interaction, perhaps due to lower water-rock ratios in this area.

Having measured the $\delta^{18}O$ of the calcite scales and of the water from which they precipitated, we can calculate the isotope fractionation factor, α (Kim and O'Neil, 1997), of each sample. Because I do not know the specific source of each calcite scale, I have used the average $\delta^{18}O$ value for the five production wells (-14.3 ± 0.2 ‰; 1 standard deviation) in this calculation. Using the average temperature recorded at the power plant intake, 164 °C, I have plotted the scale data against Eq. 1 describing equilibrium oxygen isotope fractionation between calcite and water at low temperatures, plotting $1000\ln\alpha$ vs. $10^3/T$ to allow a linear representation of the equation (Figure 9). My samples do not plot as predicted by Eq. 1. Assuming that the recorded well water temperature is the calcite precipitation temperature, calcite samples precipitated in equilibrium would be expected to have lower fractionation factors and be more depleted in ^{18}O

than our samples. This increased enrichment of ^{18}O is consistent with calcite precipitating due to a boil event, either at equilibrium but at lower temperature than 164 °C, or out of isotopic equilibrium due to rapid CO_2 loss during boiling.

6.2 Calcite $\delta^{18}O$, $\delta^{13}C$ and Δ_{47} values

As with the production well $\delta^{18}O$ data, the bulk stable isotope composition of the calcite scale chips all fall within a fairly narrow range (Figure 10). I have included the $\delta^{13}C$ and $\delta^{18}O$ data collected during clumped isotope analysis of SC03 and SC05 for comparison. This similarity is consistent with the scale samples being precipitated by a similar process or in a similar location even if they were mobilized to the screen at different times (as indicated by degree of rounding, Figure 6).

Eq. 3 produces Δ_{47}-based apparent temperatures for scale samples SC03 and SC05 of 205 ± 27 °C and 185 ± 28 °C respectively. These are both higher than the recorded temperature at the plant intake (164°C), although given the analytical and calibration uncertainties, the Δ_{47}-based apparent temperature of SC05 is just within error of the plant intake water temperature at the 95% confidence level. For the observed intake water temperature, following the calibration curves of Kluge et al. (2015), we would expect a higher per mil of ^{18}O-^{13}C clumps (in the absolute reference frame; Figure 11); in other words, the higher than expected apparent Δ_{47} temperatures indicate that that observed Δ_{47} values are lower than expected for calcite precipitating at equilibrium from 164°C water. These higher apparent Δ_{47} temperatures are inconsistent with equilibrium precipitation of calcite from cooler-than-164°C waters due to boiling. I have also applied Eq. 1 using these apparent Δ_{47}-based temperatures and the measured calcite $\delta^{18}O$ values to predict the $\delta^{18}O$ of the water. These calculated $\delta^{18}O$ of water values, -9.3 ± 0.5 ‰ for SC03 and -9.6 ± 1.9 ‰ for SC05 (Table 2) are higher than the measured $\delta^{18}O$ values of the production well waters (Table 2) by roughly 4 to 5 ‰. This exercise shows that the combined calcite $\delta^{18}O$ and Δ_{47} data are inconsistent with equilibrium calcite growth from waters that are similar to the modern brines I sampled.

6.3 Potential for disequilibrium scale calcite growth

Apparent temperatures calculated from the $\delta^{18}O$ fractionation factors (Eq. 1), 152 ± 1 °C for SC03 and 140 ± 1 °C for SC05, under-predict the observed temperatures while the Δ_{47} data over-

predict them (Figure 12). Some of the measured waters have low pH values (as low as 5.7); although low precipitating solution pH can influence calcite Δ_{47} values, we would expect a *decrease* in apparent Δ_{47} temperatures due to this effect (Hill et al., 2014). This is the opposite of what we observe, and pH is therefore not responsible for the discrepancy. The δ^{18}O-temperature relationship of Kim and O'Neil (1997) was developed using experiments at lower temperature (10, 25 and 40 °C) than are recorded for this geothermal system, so it is possible that extrapolation errors may account for some of the discrepancy between the two thermometers. However, extrapolations cannot explain such a large discrepancy, suggesting that the calcite scale did not grow at isotopic equilibrium from modern well waters at the modern water intake temperature.

It is possible the calcite grew at equilibrium from water with a different temperature and isotopic composition than the average modern well waters. Calculations in section 6.2 show that the measured Δ_{47} and calcite δ^{18}O values would be consistent with equilibrium calcite precipitation from water with a δ^{18}O value of around -9 or -10 ‰, at elevated temperatures of around 185-200 °C. This δ^{18}O water value falls between the average well water δ^{18}O value of around -14 ‰ and the -7.6 ‰ δ^{18}O value of well sample MW6, and is therefore not entirely unreasonable. But this scenario is unlikely given that the similarity of the scale calcite δ^{18}O and δ^{13}C values would then require that all of the samples grew from waters with anomalously high δ^{18}O values, and also anomalously high water temperatures. Higher well temperatures in this range have been observed in the past, but subsurface water temperatures circulating in the time since the scale likely grew are much lower than would be required by this scenario. To represent equilibrium precipitation at such high temperatures and from elevated δ^{18}O waters, the samples would have had to grow years ago before water temperatures in the field cooled, and only recently be broken off and transported to the sampling sites.

Alternatively, if boiling and associated rapid CO_2 degassing influenced scale growth, the measured Δ_{47} and calcite δ^{18}O values may indicate some amount of isotopic disequilibrium. Theoretical modeling of rapidly degassing carbonate solutions indicates that kinetic isotope fractionation can occur, increasing carbonate δ^{18}O while decreasing the Δ_{47} value (Guo, 2008). In an attempt to further characterize the influence of boiling on the scale precipitation, I compared (1) the δ^{18}O$_{water}$ value as calculated from a water temperature of 164 °C and the measured calcite

$\delta^{18}O$ data to the average $\delta^{18}O_{water}$ for the wells and (2) the Δ_{47} data recorded for SC03 and SC05 to the expected Δ_{47} value for water at 164 °C (average temperature of production wells). If 164 °C was indeed the temperature of calcite growth, our samples show a ~0.01 ‰ decrease in Δ_{47} for a ~1 ‰ increase in $\delta^{18}O$, which is smaller but a similar order of magnitude to the relative offset predicted by Guo (2008) for calcites precipitated under disequilibrium conditions due to rapid CO_2 degassing. This lends support to the idea that the samples may record some degree of non-equilibrium growth.

Given that the plant is known to occasionally experience loss of the positive pressure used to control boiling due to plant shutdown events, it is probable that the calcite scale samples that I collected all precipitated as a result of boiling within the system. As discussed in section 3.2, during such depressurization/boil events, calcite precipitates rapidly due to CO_2 degassing. This sort of rapid precipitation of my samples is supported by the uniformity of the bulk isotope date for the scale samples. Particularly, if the scale grew from waters similar in temperature and O isotopic composition to the average well waters I sampled, the calcite $\delta^{18}O$ and Δ_{47} values are consistent with direction and approximate magnitude of ^{18}O enrichment and Δ_{47} depletion that would accompany kinetic isotope effects due to rapid CO_2 degassing associated with boiling.

7 Conclusion

I have estimated the precipitation temperatures of two calcite samples from within a geothermal energy production facility by two different methods. Both methods, based on the isotopic composition of CO_2 generated from acid digestion of the samples, vary from the recorded temperature of the system. These deviations from the known temperature may stem from disequilibrium within the system resulting from the plant shutdown events. Analyzing more of the scale samples for Δ_{47} would allow for more robust statistical analysis which could allow for a stronger statement about the nature of the difference between the recorded system temperature and the temperatures calculated from clumped isotope thermometry. Other work that could improve our understanding of this system includes modeling water-rock interactions in the system (e.g., Banner and Hanson, 1990; Huntington et al., 2011; Huntington and Lechler, 2015) incorporating the geochemistry of the reservoir rock in the $\delta^{18}O$ analysis of the brine and other water wall samples. It is possible that oxygen isotopes are being exchanged in quantities large enough to impact the water chemistry. This is particularly true of the sample from MW6. Also,

developing a method by which calcite scale could be sampled in situ, and not as collected from the filter screen, would allow for direct comparison between production well waters and scale precipitating from them. This would, again, increase the certainty with which statements could be made about what is causing the calcite precipitation and how closely the theoretical system matches the actual system.

8 References

AltaRock Energy, Inc., 2014, 2013-2014 Blue Mountain Reservoir Management Report:.

Banner, J.L., and Hanson, G.N., 1990, Calculation of simultaneous isotopic and trace element variations during water-rock interaction with applications to carbonate diagenesis: Geochimica et Cosmochimica Acta, v. 54, p. 3123–3137, doi: 10.1016/0016-7037(90)90128-8.

Browne, P.R.L., and Ellis, A.J., 1970, The Ohaki-Broadlands hydrothermal are, New Zealand: Minerlogy and related geochemistry: American Journal of Science, v. 269, p. 97–131.

Coplen, T.B., 1993, Reporting of stable carbon, hydrogen, and oxygen isotopic abundances, *in* Reference and intercomparison materials for stable isotopes of light elements, p. 31–34.

Dennis, K.J., Affek, H.P., Passey, B.H., Schrag, D.P., and Eiler, J.M., 2011, Defining an absolute reference frame for "clumped" isotope studies of CO 2: Geochimica et Cosmochimica Acta, v. 75, p. 7117–7131, doi: 10.1016/j.gca.2011.09.025.

Dennis, K.J., and Schrag, D.P., 2010, Clumped isotope thermometry of carbonatites as an indicator of diagenetic alteration: Geochimica et Cosmochimica Acta, v. 74, p. 4110–4122, doi: 10.1016/j.gca.2010.04.005.

Eiler, J.M., 2007, " Clumped-isotope " geochemistry — The study of naturally-occurring , multiply-substituted isotopologues: Earth and Planetary Science Letters, v. 262, p. 309–327, doi: 10.1016/j.epsl.2007.08.020.

Eiler, J.M., and Schauble, E., 2004, 18O13C16O in Earth's atmosphere: Geochimica et Cosmochimica Acta, v. 68, p. 4767–4777, doi: 10.1016/j.gca.2004.05.035.

Epstein, S., and Mayeda, T., 1953, Variation of O18 content of waters from natural sources: Geochimica et Cosmochimica Acta, v. 4, p. 213–224, doi: 10.1016/0016-7037(53)90051-9.

Faulds, J.E., and Melosh, G., 2008, A Preliminary Structural Model for the Blue Mountain Geothermal Field, Humboldt County, Nevada: GRC Transactions, v. 32, p. 273–278.

Ghosh, P., Adkins, J., Affek, H., Balta, B., Guo, W., Schauble, E.A., Schrag, D., and Eiler, J.M., 2006, 13C–18O bonds in carbonate minerals: A new kind of paleothermometer: Geochimica et Cosmochimica Acta, v. 70, p. 1439–1456, doi: 10.1016/j.gca.2005.11.014.

Guo, W., 2008, Carbonate clumped isotope thermometry : application to carbonaceous chondrites and effects of kinetic isotope fractionation: California Institute of Technology.

Gupta, P., Noone, D., Galewsky, J., Sweeney, C., and Vaughn, B.H., 2009, Demonstration of high-precision continuous measurements of water vapor isotopologues in laboratory and remote field deployments using wavelength-scanned cavity ring-down spectroscopy (WS-CRDS) technology.: Rapid communications in mass spectrometry : RCM, v. 23, p. 2534–42, doi: 10.1002/rcm.4100.

Hill, P.S., Tripati, A.K., and Schauble, E.A., 2014, Theoretical constraints on the effects of pH, salinity, and temperature on clumped isotope signatures of dissolved inorganic carbon species and precipitating carbonate minerals: Geochimica et Cosmochimica Acta, v. 125, p.

610–652, doi: 10.1016/j.gca.2013.06.018.

Huntington, K.W., Budd, D.A., Wernicke, B.P., and Eiler, J.M., 2011, Use of Clumped-Isotope Thermometry To Constrain the Crystallization Temperature of Diagenetic Calcite: Journal of Sedimentary Research, v. 81, p. 656–669, doi: 10.2110/jsr.2011.51.

Huntington, K.W., and Lechler, A.R., 2015, Carbonate clumped isotope thermometry in continental tectonics: Tectonophysics, v. 647-648, p. 1–20, doi: 10.1016/j.tecto.2015.02.019.

IAEA/WMO, 2016, Global Network of Isotopes in Precipitation: The GNIP Database,.

Kim, S.-T., and O'Neil, J.R., 1997, Equilibrium and nonequilibrium oxygen isotope effects in synthetic carbonates: Geochimica et Cosmochimica Acta, v. 61, p. 3461–3475, doi: 10.1016/S0016-7037(97)00169-5.

Kluge, T., John, C.M., Jourdan, A.L., Davis, S., and Crawshaw, J., 2015, Laboratory calibration of the calcium carbonate clumped isotope thermometer in the 25-250°C temperature range: Geochimica et Cosmochimica Acta, v. 157, p. 213–227, doi: 10.1016/j.gca.2015.02.028.

McCrea, J.M., 1950, On the Isotopic Chemistry of Carbonates and a Paleotemperature Scale: The Journal of Chemical Physics, v. 18, p. 849, doi: 10.1063/1.1747785.

Passey, B.H., and Henkes, G.A., 2012, Carbonate clumped isotope bond reordering and geospeedometry: Earth and Planetary Science Letters, v. 351-352, p. 223–236, doi: 10.1016/j.epsl.2012.07.021.

Satman, A., Ugur, Z., and Onur, M., 1999, The effect of caclite deposition on geothermal well inlow performance: Geothermics, v. 28, p. 425–444.

Schauble, E.A., Ghosh, P., and Eiler, J.M., 2006, Preferential formation of 13 C – 18 O bonds in carbonate minerals , estimated using first-principles lattice dynamics: Geochimica et Cosmochimica Acta, v. 70, p. 2510–2529, doi: 10.1016/j.gca.2006.02.011.

Simmons, S.F., and Christenson, B.W., 1994, Origins of calcite in a boiling geothermal system: American Journal of Science, v. 294, p. 361–400, doi: 10.2475/ajs.294.3.361.

Sumner, K.K., Camp, E.R., Huntington, K.W., Cladouhos, T.T., and Uddenberg, M., 2015, Assessing Fracture Connectivity using Stable and Clumped Isotope Geochemistry of Calcite Cements, *in* Fortieth Workshop on Geothermal Reservoir Engineering, Stanford, CA, p. 1–12.

Tang, J., Dietzel, M., Fernandez, A., Tripati, A.K., and Rosenheim, B.E., 2014, Evaluation of kinetic effects on clumped isotope fractionation (δ47) during inorganic calcite precipitation: Geochimica et Cosmochimica Acta, v. 134, p. 120–136, doi: 10.1016/j.gca.2014.03.005.

The Weather Company, L., 2016, Weather History for Winnemucca, NV: Weather Underground,.

Tobin, T.S., Schauer, A.J., and Lewarch, E., 2011, Alteration of micromilled carbonate δ18O during Kiel Device analysis.: Rapid communications in mass spectrometry : RCM, v. 25, p. 2149–52, doi: 10.1002/rcm.5093.

Urey, H.C., 1947, The thermodynamic properties of isotopic substances: Journal of the Chemical Society (Resumed), p. 562, doi: 10.1039/jr9470000562.

Wyld, S.J., 2002, Structural evolution of a Mesozoic backarc fold-and-thrust belt in the U . S . Cordillera : New evidence from northern Nevada: Geological Society of America Bulletin, p. 1452–1468.

Table 1. $\delta^{18}O$ data for water samples given in per mil (‰) and referenced to Standard Mean Ocean Water (VSMOW). The first five samples are from production wells. The Common Injection sample was collected from the common effluent line from the Ormat generators before the flow is divided between the injection wells. The MW# samples and WW5 are from monitoring wells screened at various depths around the geothermal field. WW14 and WW18 are shallow aquifer wells that supply cooling water to the plant. The puddle sample was collected from surface water on the flank of Blue Mountain (Figure 1), presumably meteoric in origin.

Sample	$\delta^{18}O$ (‰), (VSMOW)	Std dev	Temperature (°C)	pH	Well Type
14-14	-14.87	0.06	161*, 22.3**	5.70	Production
17-14	-13.87	0.06	168*, 41.2**	5.78	Production
23-14	-14.29	0.07	161*, 21.3**	5.63	Production
25-14	-14.75	0.12	166*, 26.4**	5.68	Production
26A-14	-13.95	0.07	164*, 33.4**	5.71	Production
Common Injection	-14.81	0.07	64*, 35.4**	5.74	Injection
MW5	-15.14	0.06	30.7**	6.48	Monitoring
MW6	-7.57	0.07	20.1**	6.71	Monitoring
MW7	-14.87	0.04	21.7**	6.02	Monitoring
WW5	-15.04	0.05	45.0**	6.51	Monitoring
WW14	-15.24	0.04	24.8**	7.04	Cold water
WW8	-15.26	0.06	21.2**	7.14	Cold water
Puddle	-6.69	0.04	10.8**	8.43	---

* denotes temperatures from production system monitoring by AltaRock.

** denotes temperatures recorded at time of sampling.

Table 2 Stable isotope data for calcite samples. Measured values are referenced to Vienna Pee Dee Belemnite (VPDB). Scale samples SC01 - SC10 were collected at random from scale material removed from the filter screen before the power generators. Each SC# sample is presented as the average of values from subsamples taken from the pipe-side and flow-side of each chip. The samples were tested this way in order to determine whether or not the calcite had experienced multiple generations of precipitation. The individual results, presented in Appendix I, indicate that the chips did not experience generational precipitation.

Sample	$\delta^{13}C$ (‰), (VPDB)	$\delta^{13}C$ (‰), Std error	$\delta^{18}O_{CaCO3}$ (‰), (VPDB)	$\delta^{18}O_{CaCO3}$ (‰), Std error	Δ_{47} (‰) ARF	Δ_{47} (‰) Std error	T(Δ_{47}) (°C), (Kluge, 2015)	$\delta^{18}O_{H2O}$ (‰), (VSMOW), (Kim & ONeil, 1997)
SC01	-8.45	0.07	-34.17	0.11				
SC02	-8.52	0.13	-33.87	0.26				
SC03	-8.61	0.04	-33.89	0.11	0.344	0.015	205 ± 27	-9.26 ± 0.51
SC04	-8.54	0.08	-33.92	0.18				
SC05	-8.07	0.07	-32.67	0.12	0.360	0.018	185 ± 28	-9.62 ± 1.93
SC06	-8.33	0.04	-33.59	0.35				
SC07	-8.33	0.05	-33.47	0.41				
SC08	-8.42	0.12	-33.53	0.29				
SC09	-8.18	0.11	-33.31	0.06				
SC10	-8.09	0.24	-33.02	0.92				
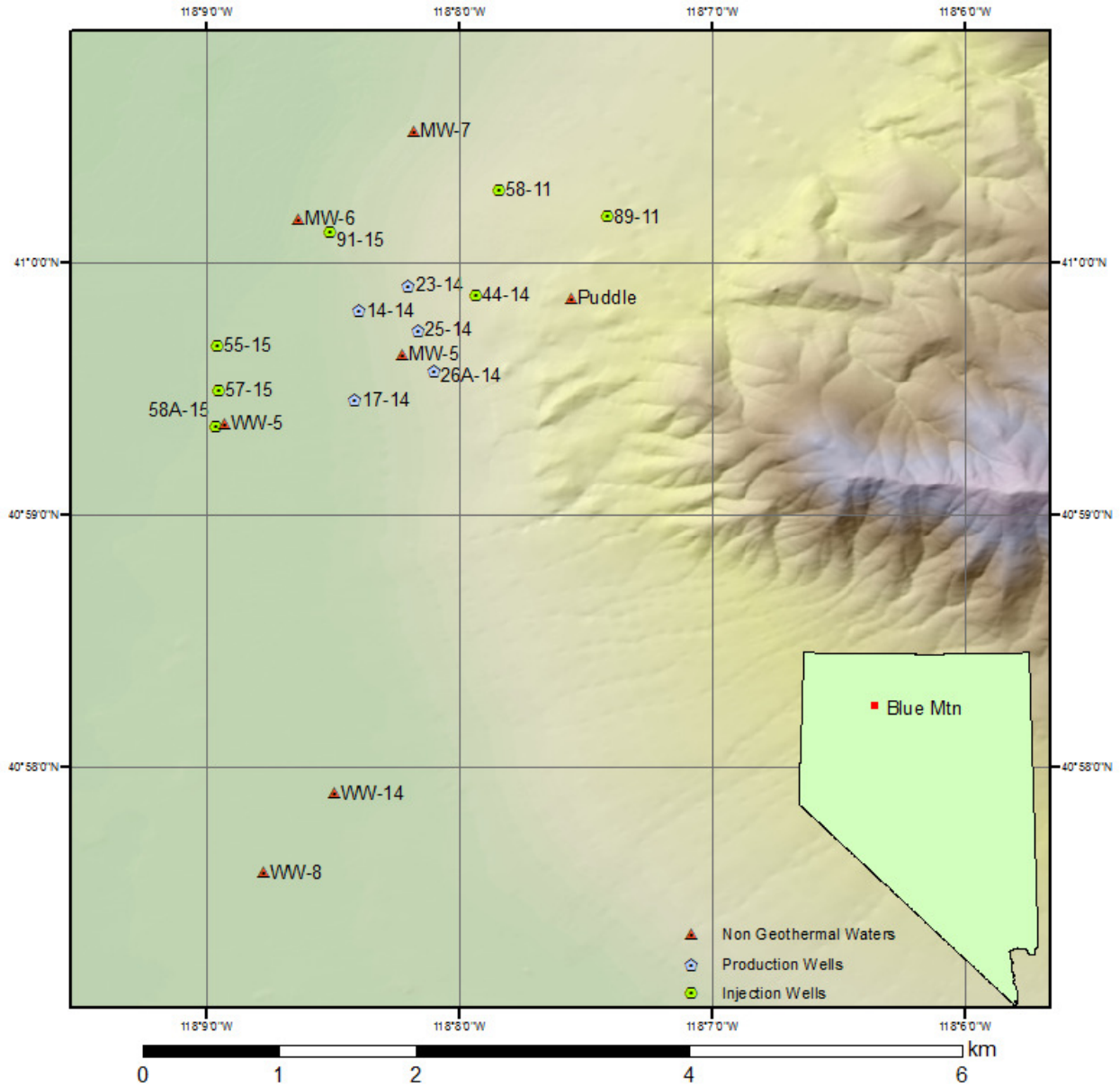
Figure 1. Location map showing location of water sample locations. Well locations courtesy of AltaRock Energy, Inc. Nevada DEM from The National Map courtesy of the U.S. Geological Survey <http://viewer.nationalmap.gov/launch/>
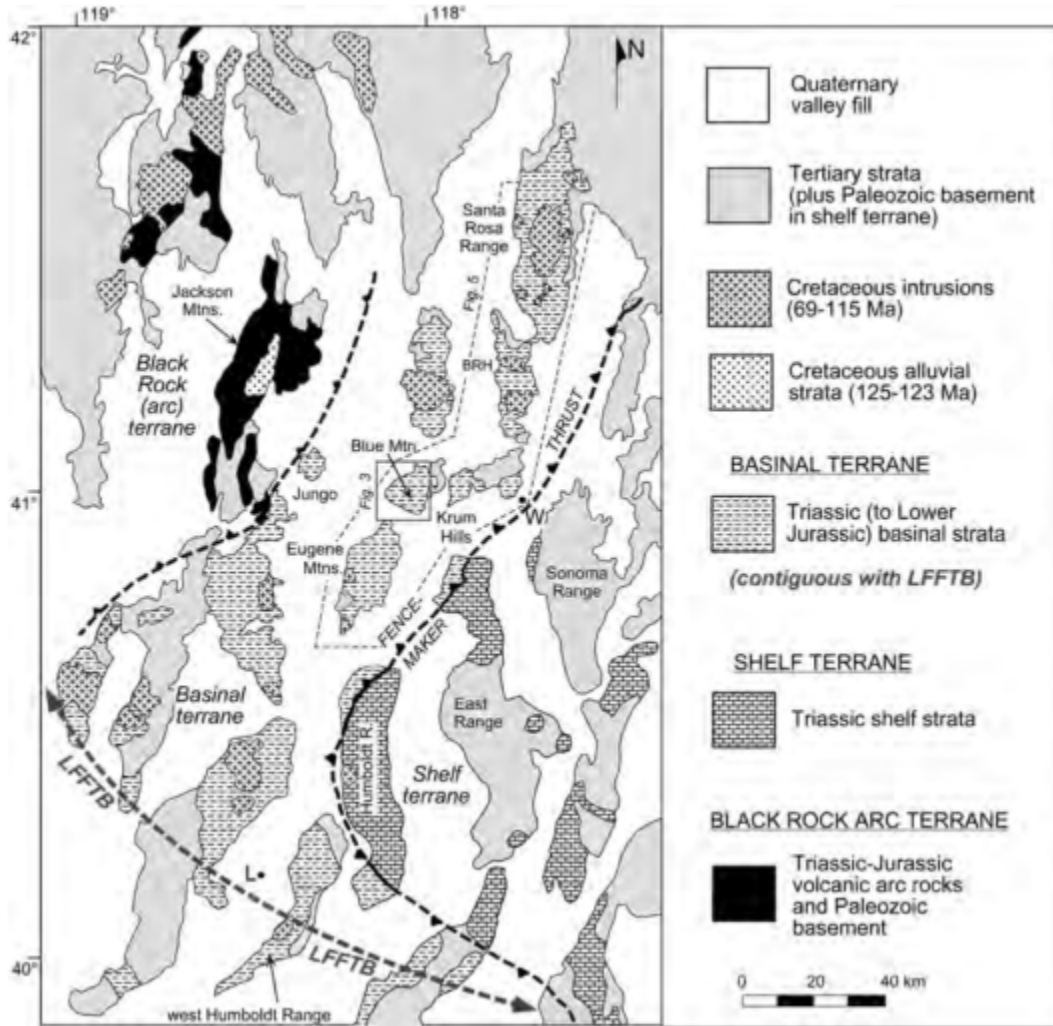
Figure 2. Geology and general structure in the vicinity of Blue Mountain. (Wyld, 2002).
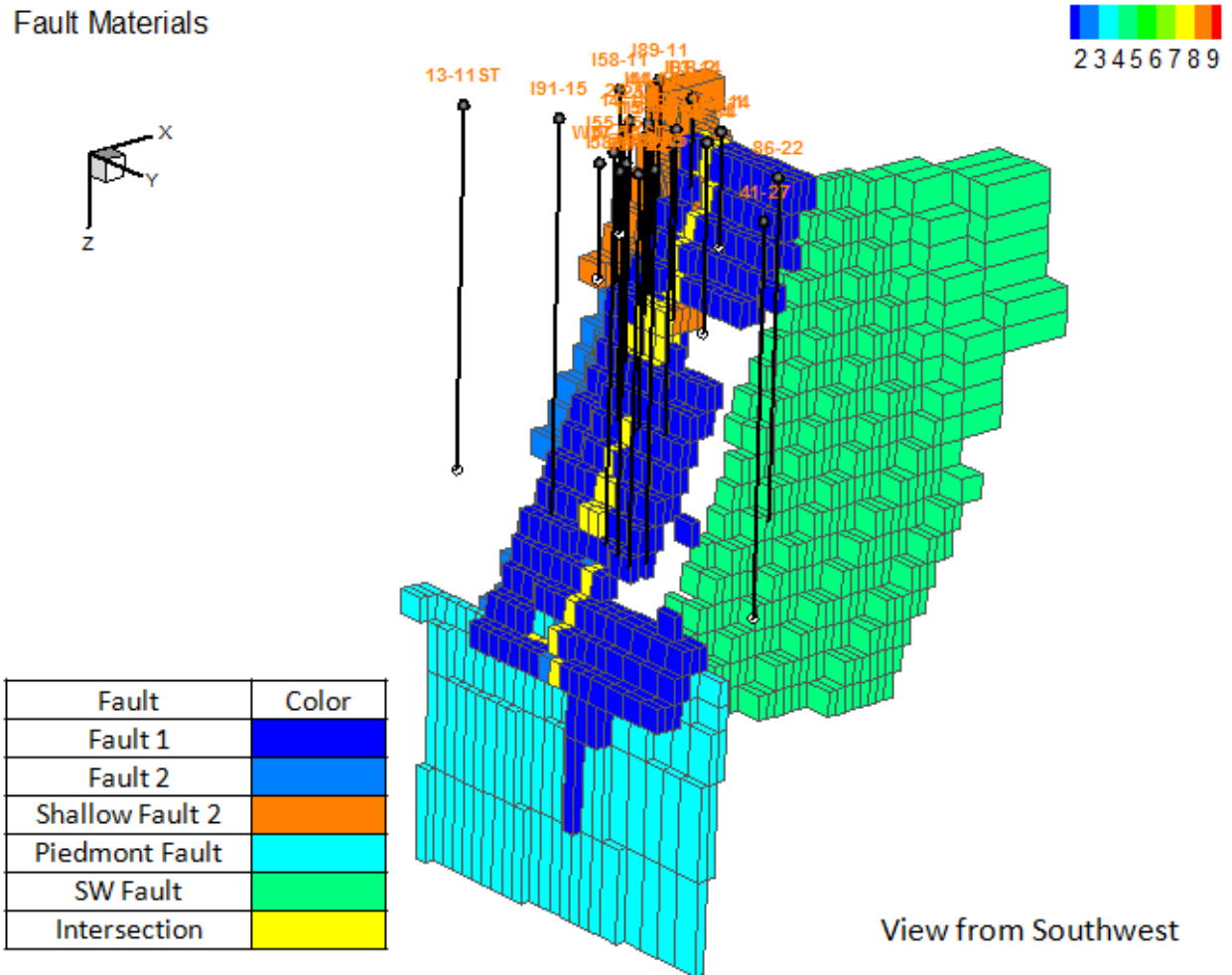
Figure 3. Western dipping faults that compose the primary geothermal aquifer at Blue Mountain. Image courtesy of AltaRock Energy, Inc.

Common plant inflow from 5 production wells

Filter screen location

Power generators

Gen. 1

Gen. 2

Gen. 3

Approx. sample location

Common plant outflow to 7 injection wells
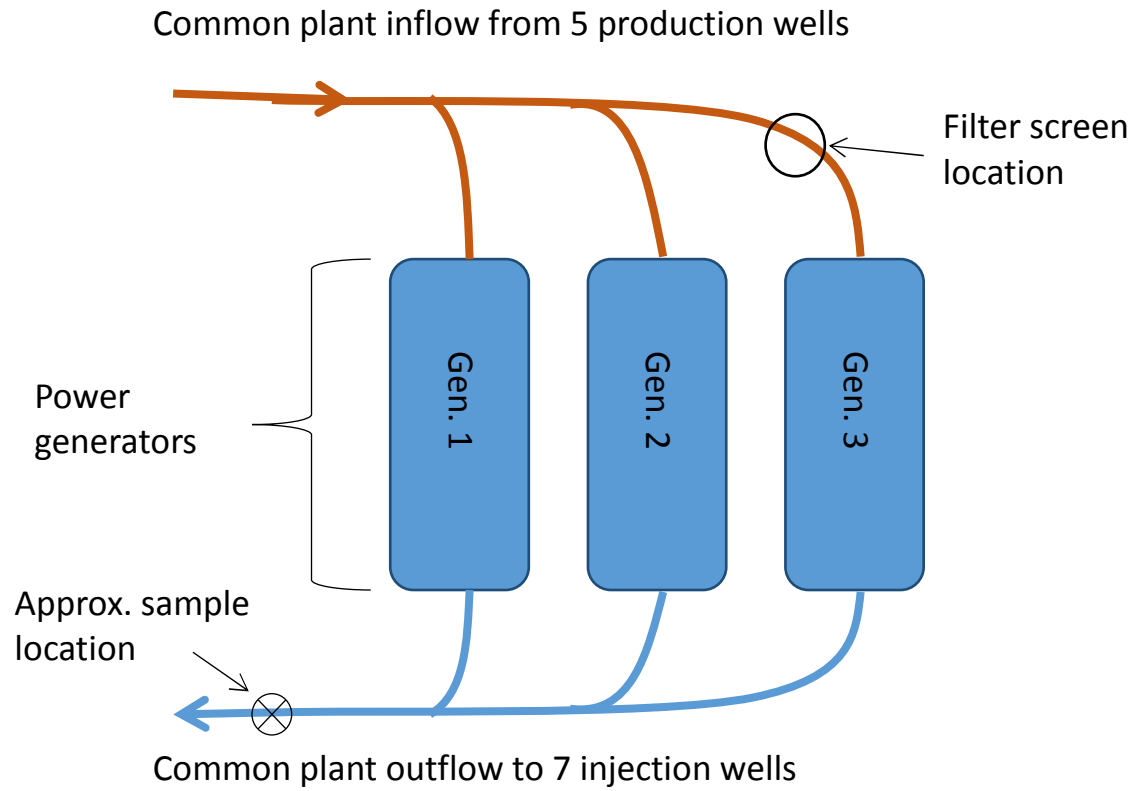
Figure 4. Simplified schematic of water flow through power plant. For more detail, see Appendix 4.

Figure 5. (a) Assembly used to cool production well brine to manageable temperatures for sampling while preventing boiling. Drum is filled with cool tap-water. (b) Cooling coil from within sampling assembly.

Figure 6. Scale chips collected from filter screen in place to prevent large material from entering Ormat power generators. Chips were chosen at random. Pieces exhibiting more rounding have likely been trapped in the screen longer than those with sharper edges.

Figure 7. Material that has precipitated around a leak in the pump housing at production well 14-14. The red dashed circle indicates the approximate location where sample calcite sample 14-14 was collected. The source/cause of the staining is unknown; however, one possibility is the oil used to lubricate the pump shaft. The amount of CO_2 released during phosphoric acid digest indicates that it is 0.25% pure carbonate.
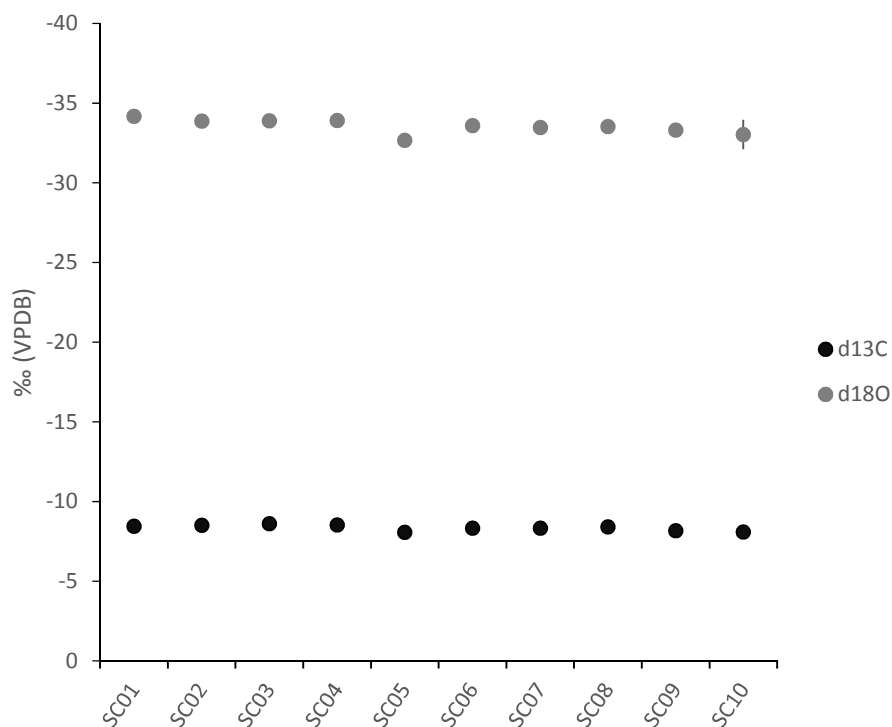
Figure 8. Bulk isotope values for calcite scale samples as referenced against VPDB. $\delta^{13}C$ values range from -8.606 to -8.072 ‰. $\delta^{18}O$ values range from -34.167 to –33.022 ‰. Error bars representing standard error between replicates (analytical samples derived from front and back of each scale chip) are present on each point. However, with the exception of the $\delta^{18}O$ value for SC10, the errors are small enough that they are not visible behind the data markers (0.041 to 0.41 ‰).
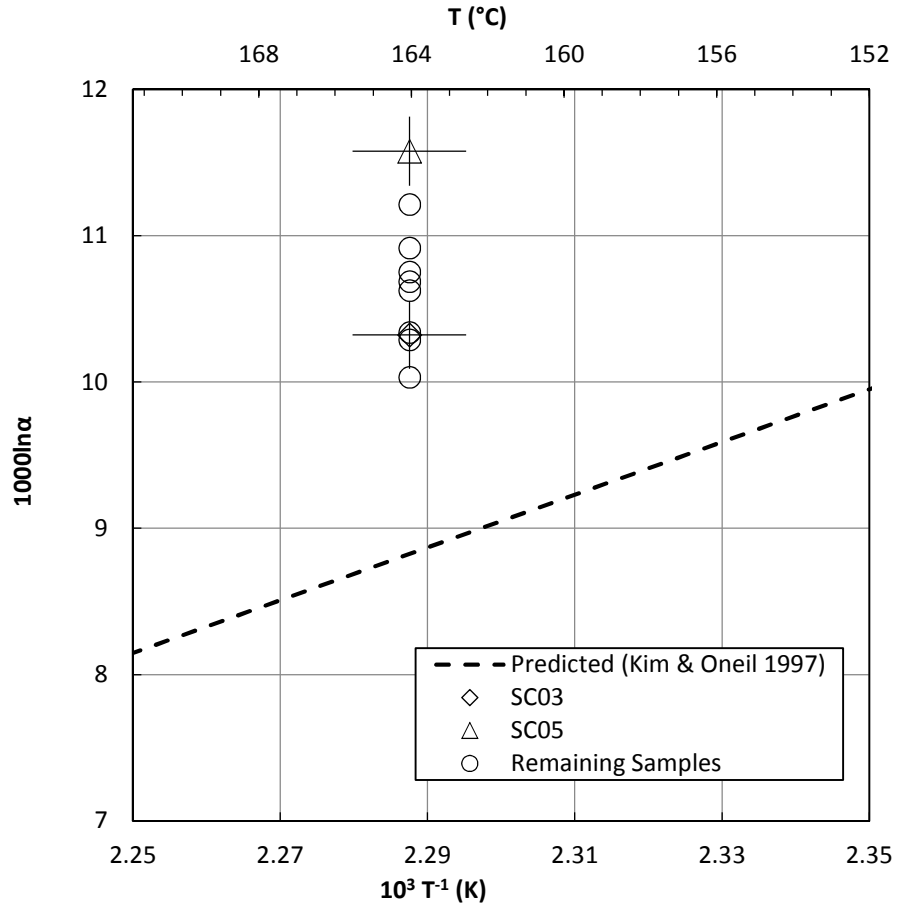
Figure 9. The fractionation factors calculated from the $\delta^{18}O$ stable isotope data for the calcite scale samples and the average $\delta^{18}O$ value for the production wells plotted against the recorded average temperature of the production wells. The data plot above the function predicted by Kim and O'Neil (1997); calcite precipitated in equilibrium with ~164 °C well water with water $\delta^{18}O$ values of -13.87 to -15.26 ‰ would be more depleted in ^{18}O than the scale samples. Error bars represent standard error of $\delta^{18}O$ measurements and standard error of temperatures recorded at each of the production wells.
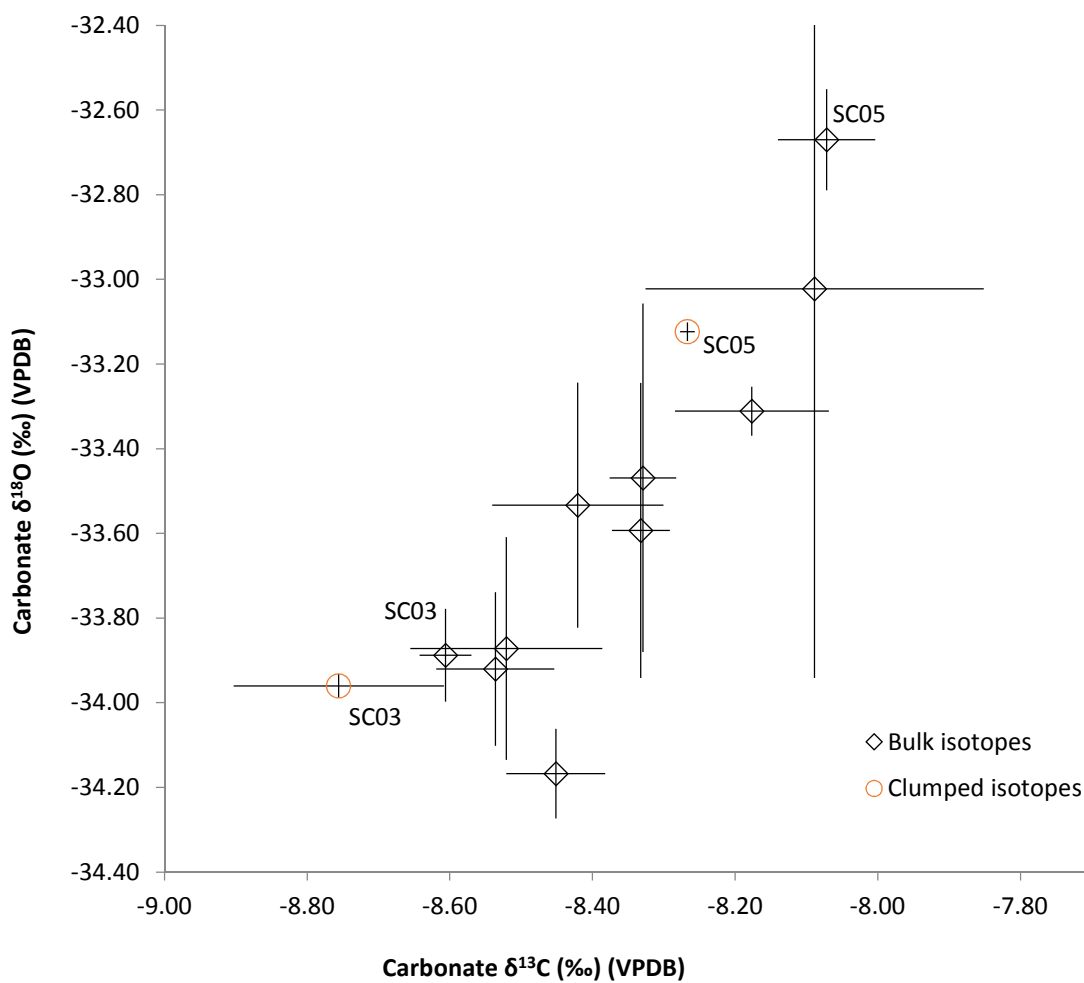
Figure 10. Comparison between bulk isotope data collected from Finnigan Delta Plus ($\delta^{18}O$ and $\delta1^3C$ only) and isotope date collected from Thermo MAT253 ($\delta^{18}O$ and $\delta^{13}C$ measurements accompanying Δ_{47}). Error bars represent standard error of replicates.
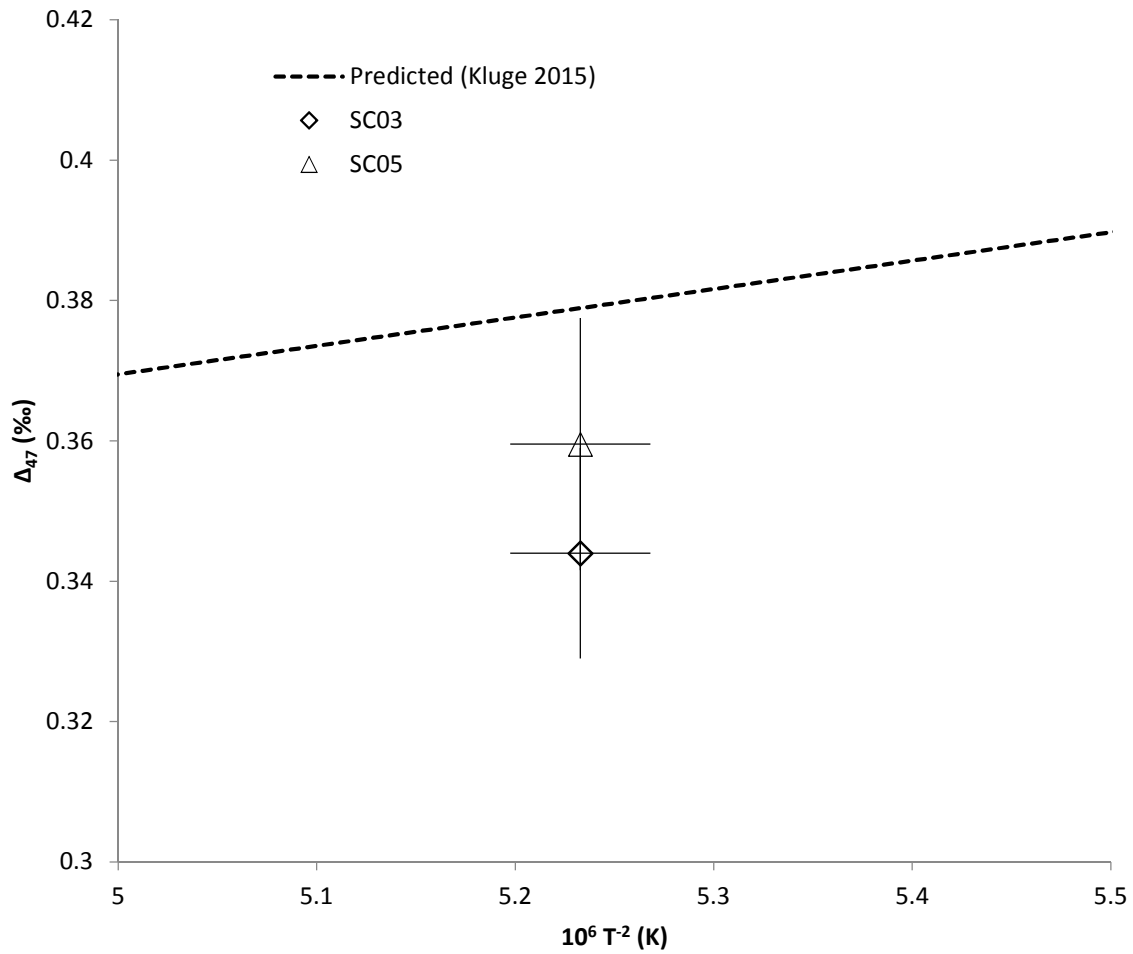
Figure 11. Δ_{47} data of SC03 and SC05 plotted with known temperature against the temperature calibration of Kluge et al. (2015). Temperature is plotted as the function $10^6/T^2$ to allow for a linear plot. Error bars represent standard error of three replicates for each Δ_{47} measurements and standard error of temperatures recorded at each of the production wells.
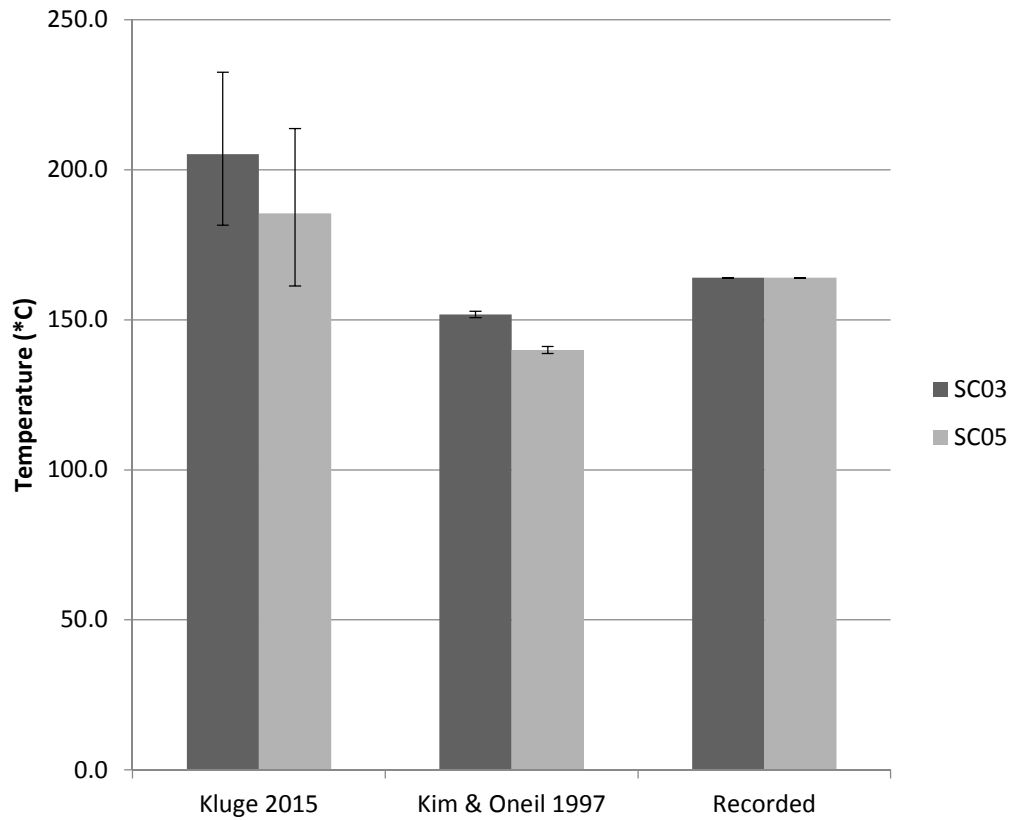
Figure 12. Temperatures derived from Δ_{47} (Kluge et al., 2015) and from $\delta^{18}O$ of calcite and water (Kim and O'Neil, 1997) for scale samples SC03 and SC05 as compared to the average intake temperatures recorded for the power plant. Errors for Δ_{47} temperatures were derived from both analytical error and calibration error inherent in the relationship. Error for $\delta^{18}O$ temperatures were calculated using analytical error.

Appendix I: Water $\delta^{18}O$ results

Sample Name	Mean H$_2$O qty ppmv	StdDev H$_2$O qty ppmv	Mean δD	StdDev δD	Mean $\delta^{18}O$	StdDev $\delta^{18}O$
14-14	18773.4567	77.2728	-131.3096	0.14363	-14.8724	0.062079
17-14	19070.434	92.0429	-125.3856	0.13506	-13.8707	0.058343
23-14	19159.6513	86.9675	-127.9742	0.23784	-14.2912	0.071609
25-14	18828.0331	102.4823	-130.2798	0.4864	-14.7531	0.11583
26A-14	18683.2417	85.4423	-125.5847	0.085554	-13.9484	0.071098
COMMON INJECTION	18875.5704	55.484	-130.963	0.28615	-14.8103	0.068414
MW5	19135.9861	67.8818	-131.0995	0.18085	-15.144	0.064101
MW6	19010.3756	120.3029	-77.1803	0.15069	-7.5736	0.072539
MW7	19038.2469	54.8021	-132.0486	0.33661	-14.8724	0.036464
WW5	19198.781	100.7918	-131.5286	0.11508	-15.0409	0.045408
WW14	19251.8681	57.7536	-125.7196	0.1066	-15.2419	0.043821
WW8	19169.5627	104.3156	-123.4327	0.16994	-15.2616	0.059313
PUDDLE	19028.3704	125.6546	-74.0804	0.24273	-6.6939	0.039711

Appendix II: Calcite $\delta^{13}C$ and $\delta^{18}O$ results

Sample	Time in Kiel (days)	Sample mass (mg)	Total CO₂ (mbar)	Percent carbonate	Mean $\delta^{13}C$ vs VPDB (‰)	StdDev $\delta^{13}C$ (‰)	Accuracy $\delta^{13}C$ (‰)	Precision $\delta^{13}C$ (‰)	Mean d $\delta^{18}O$ vs VPDB (‰)	StdDev $\delta^{18}O$ (‰)	Accuracy $\delta^{18}O$ (‰)	Precision $\delta^{18}O$ (‰)
14-14	0.30442	0.106	335	21.790566	-17.691	0.226	-0.01696	0.08677	-13.9607	0.222	-0.05289	0.058261
sc01a	0.32487	0.101	1101	101.52475	-8.5207	0.013	-0.01696	0.08677	-34.0615	0.023	-0.05289	0.058261
sc01b	0.34524	0.092	1177	124.30435	-8.382	0.01	-0.01696	0.08677	-34.2734	0.02	-0.05289	0.058261
sc02a	0.3678	0.097	1203	122.2268	-8.3861	0.014	-0.01696	0.08677	-33.609	0.024	-0.05289	0.058261
sc02b	0.38914	0.104	1097	98.019231	-8.6552	0.013	-0.01696	0.08677	-34.1348	0.013	-0.05289	0.058261
sc03a	0.41565	0.1	1146	109.45	-8.6422	0.01	-0.01696	0.08677	-33.9971	0.02	-0.05289	0.058261
sc03b	0.43443	0.101	1057	95.078218	-8.5699	0.01	-0.01696	0.08677	-33.7783	0.015	-0.05289	0.058261
sc04a	0.45517	0.107	1132	100.26168	-8.6191	0.013	-0.01696	0.08677	-34.1021	0.024	-0.05289	0.058261
sc04b	0.54417	0.099	1191	117.78788	-8.4534	0.01	-0.01696	0.08677	-33.7387	0.014	-0.05289	0.058261
sc05a	0.56516	0.112	1124	94.6875	-8.0034	0.009	-0.01696	0.08677	-32.5485	0.017	-0.05289	0.058261
sc05b	0.58638	0.11	1149	99.927273	-8.14	0.009	-0.01696	0.08677	-32.7872	0.015	-0.05289	0.058261
sc06a	0.60719	0.111	1185	104.18018	-8.2916	0.014	-0.01696	0.08677	-33.2446	0.014	-0.05289	0.058261
sc06b	0.633	0.099	1103	103.88889	-8.373	0.012	-0.01696	0.08677	-33.9417	0.026	-0.05289	0.058261
sc07a	0.65344	0.109	1221	111.48624	-8.2826	0.023	-0.01696	0.08677	-33.0575	0.027	-0.05289	0.058261
sc07b	0.67564	0.117	1235	105.8547	-8.376	0.016	-0.01696	0.08677	-33.8803	0.032	-0.05289	0.058261
sc08a	0.69633	0.114	1140	95.192982	-8.5407	0.006	-0.01696	0.08677	-33.8229	0.023	-0.05289	0.058261
sc08b	0.78476	0.092	965	90.407609	-8.3007	0.014	-0.01696	0.08677	-33.2436	0.021	-0.05289	0.058261
sc09a	0.80604	0.117	1137	92.350427	-8.2846	0.012	-0.01696	0.08677	-33.2535	0.028	-0.05289	0.058261
sc09b	0.82806	0.097	1213	123.91753	-8.0687	0.012	-0.01696	0.08677	-33.3694	0.021	-0.05289	0.058261
sc10a	0.85583	0.109	1270	119.06422	-7.8517	0.013	-0.01696	0.08677	-32.103	0.008	-0.05289	0.058261
sc10b	0.87573	0.112	1168	100.82143	-8.3258	0.024	-0.01696	0.08677	-33.9417	0.017	-0.05289	0.058261

All samples were run assuming mineralogy was 100% pure calcite. However, analysis showed that sample 14-14 was only 20% pure calcite. Because of this impurity, and the failure to account for the impurity during analysis, results for sample 14-14 likely contain considerable analytical error and have been disregarded for the purpose of this study.

Appendix III: Δ_{47} results with accompanying $\delta^{13}C$ and $\delta^{18}O$ values

Sample ID	$\delta^{13}C$ vs VPDB (via WG) (permil)	$\delta^{13}C$ vs VPDB (formal) (permil)	$\delta^{13}C$ stdev (stderr of avg)	$\delta^{18}O$ vs VPDB (via WG) (permil)	$\delta^{18}O$ vs VPDB (formal) (permil)	$\delta^{18}O$ stdev (stderr of avg)	δ_{47} vs VPDB (via WG) (permil)	δ_{47} stdev	Δ_{47} ARF acid (permil)	Δ_{47} stderr	Apparent temp °C (Kluge et al., 2015)
160122_5_SC03	-9.07	-9.05	0.0044	-34.51	-33.91	0.0075	-28.00	0.0720	0.3491	0.0097	
160122_6_SC03	-8.62	-8.59	0.0042	-34.61	-34.01	0.0066	-27.68	0.0532	0.3476	0.0069	
160122_7_SC03	-8.65	-8.62	0.0054	-34.57	-33.97	0.0067	-27.67	0.0574	0.3352	0.0076	
SC03 Average		**-8.76**	**0.15**		**-33.96**	**0.03**			**0.3440**	**0.0044**	**205.2 ± 27.3**
160124_1_SC05	-8.29	-8.26	0.0044	-33.68	-33.09	0.0076	-26.37	0.0631	0.3943	0.0082	
160124_2_SC05	-8.29	-8.26	0.0041	-33.76	-33.16	0.0077	-26.48	0.0547	0.3502	0.0074	
160124_4_SC05	-8.32	-8.29	0.0047	-33.71	-33.12	0.0060	-26.48	0.0580	0.3342	0.0078	
SC05 Average		**-8.27**	**0.01**		**-33.12**	**0.02**			**0.3595**	**0.0180**	**185.5 ±28.2**

Sample ID	δ_{48} vs VPDB (via WG) (permil)	δ_{48} stdev	Δ_{48} (permil)	Δ_{48} stderr	δ_{49} vs VPDB (via WG) (permil)	δ_{49} stdev	Δ_{49} (permil)	Δ_{49} stderr
160122_5_SC03	-54.97	0.2733	0.7218	0.0371	1.94	18.85	59.66	2.574
160122_6_SC03	-55.23	0.2677	0.6448	0.0369	-45.81	20.19	8.90	2.756
160122_7_SC03	-55.06	0.2502	0.7345	0.0342	-3.07	18.33	54.05	2.503
160124_1_SC05	-53.06	0.2668	1.0136	0.0361	68.80	20.31	127.54	2.765
160124_2_SC05	-53.53	0.2635	0.6776	0.0364	9.42	19.60	65.06	2.669
160124_4_SC05	-53.45	0.2959	0.6600	0.0402	-5.15	17.35	49.62	2.364